

CP3: Unifying Point Cloud Completion by Pretrain-Prompt-Predict Paradigm

Mingye Xu, Yali Wang, Yihao Liu, Yu Qiao, *Senior Member, IEEE*

Abstract—Point cloud completion aims to predict complete shape from its partial observation. Current approaches mainly consist of generation and refinement stages in a coarse-to-fine style. However, the generation stage often lacks robustness to tackle different incomplete variations, while the refinement stage blindly recovers point clouds without the semantic awareness. To tackle these challenges, we unify point cloud Completion by a generic Pretrain-Prompt-Predict paradigm, namely CP3. Inspired by prompting approaches from NLP, we creatively reinterpret point cloud generation and refinement as the prompting and predicting stages, respectively. Then, we introduce a concise self-supervised pretraining stage before prompting. It can effectively increase robustness of point cloud generation, by an Incompletion-Of-Incompletion (IOI) pretext task. Moreover, we develop a novel Semantic Conditional Refinement (SCR) network at the predicting stage. It can discriminatively modulate multi-scale refinement with the guidance of semantics. Finally, extensive experiments demonstrate that our CP3 outperforms the state-of-the-art methods with a large margin.

Index Terms—Point Cloud Completion, Prompting, Self-supervised Pretraining, Semantic Refinement.



1 INTRODUCTION

Point cloud analysis has attracted a lot of research interest in computer vision and robotics. Unfortunately, the scanned point cloud is usually incomplete in practice, due to complex occlusion, light reflection, limited sensor resolution, etc. Therefore, the completion task has gradually become important. The existing approaches [1], [2], [3], [4], [5] are mainly based on point cloud generation and refinement, which first generates the coarse completion from partial point cloud, and then recovers the fine completion from the coarse one. However, these approaches focus on designing complicated models, while ignoring the fundamental problems about how to effectively use point cloud at different stages.

At the generation stage, the core problem is to learn a robust incomplete-to-complete mapping for tackling different partial observations of point cloud. Most methods mainly work on developing deterministic or probabilistic generation networks [2], [4], [5], while lacking insightful consideration about data itself. In fact, the training pairs of incomplete and complete point cloud are predetermined. With such limited data diversity, it is often difficult to generate robust completion from new incomplete variations, by training those complex generation networks from scratch. At the refinement stage, the key is to recover the plausible shape of the complete point cloud, based on the coarse (or imperfect) completion from the generation stage. However, the existing refinement approaches [4], [6], [7] ignore the semantic information of point cloud, which is an important clue of shape recovery. As a result, these refinement networks are unsatisfactory on point clouds which have similar

shapes but belong to different semantic categories, e.g., chair and table in Fig. 1.

To tackle these problems, we propose to unify point cloud Completion frameworks by a generic Pretrain-Prompt-Predict paradigm, namely CP3, which can achieve robust generation and discriminative refinement by self-supervised pretraining and semantic-guided predicting. As shown in Fig. 1, our inspiration mainly comes from the recent prompting scheme in NLP [8], [9], [10]. Specifically, as Fig. 1 shows, we flexibly reinterpret the generation stage as the prompting stage, since both stages aim at learning on new scenarios with limited data diversity. But differently, the pretrained model is ready in NLP. Therefore, its goal is to design a *prompt function* that modifies *input* as *prompt* for answer search. Alternatively, point cloud generation is not pretrained. Hence, our goal is to design an *inverse prompt function* which aims at constructing the diversified *input* from the given *prompt* (i.e., incomplete point cloud) for pretraining. In particular, we introduce a concise Incompletion-Of-Incompletion (IOI) sampling mechanism as *inverse prompt function*, where we randomly crop incomplete point clouds into new incomplete-of-incomplete ones. Subsequently, we pretrain the generation network with a self-supervised pretext task, which applies the IOI point cloud as input to recover the original incomplete point cloud. This design contains two main advantages. First, this pretraining task is similar to the downstream generation task, which can reduce the task gap for model transfer [8]. Second, IOI pretraining can effectively increase robustness of generation network, by pretraining on rich variations of incomplete point clouds.

Moreover, we reinterpret the refinement stage as the predicting stage, since this stage is used to map the imperfect point cloud (i.e., *answer of prompt*) into the refined one (i.e., the target *output*). But different from answer mapping in NLP, point cloud refinement requires extra semantic knowledge, since the shape of point cloud is highly relevant

- M. Xu, Y. Wang and Y. Liu are with Shenzhen Institute of Advanced Technology, Chinese Academy of Sciences, Shenzhen, 518055. Email: my.xu@siat.ac.cn.
- M. Xu and Y. Liu are also with the University of Chinese Academy of Sciences, Beijing, 100049. Y. Wang and Y. Qiao are with with Shanghai AI Laboratory.
- Y. Wang and Y. Qiao are co-corresponding authors.

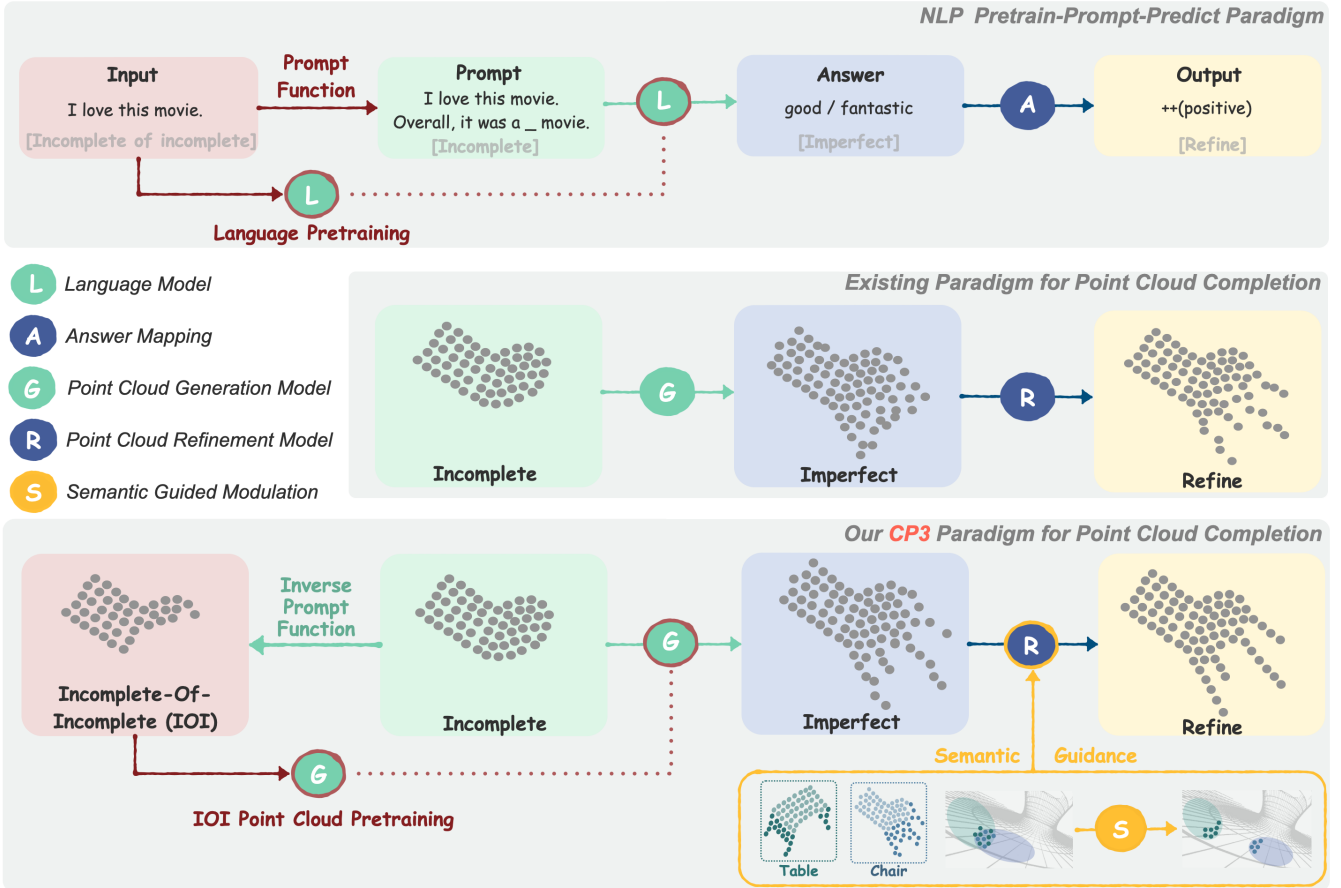


Fig. 1: Our CP3 paradigm. We unify point cloud completion by the recent prompting scheme in NLP, since we find the *incomplete* point cloud plays a similar role as the *incomplete* sentence, e.g., “I love this movie. Overall, it was a __ movie”. Following this line, we reinterpret point cloud generation and refinement as the prompting and predicting stages, which first generates the imperfect point cloud (like *answer*: “good / fantastic”) from the incomplete one, and then refines target point cloud (like *output*: “++(positive)”) from the imperfect one. But different from NLP, point cloud generation is not pretrained, and refinement lacks semantic awareness. Hence, we propose a concise IOI pretraining to boost generation robustness in a self-supervised way, and design a novel semantic guidance to modulate refinement for shape confusion reduction.

to its high-level semantics, such as category information. Based on this observation, we propose a novel Semantic Conditional Refinement (SCR) network, which adaptively leverage semantic information as discriminative guidance for refining point cloud. Specifically, it mainly consists of two distinct blocks, i.e., semantic-guided modulation and multi-scale point deconvolution blocks. The semantic-guided modulation block smartly converts the semantic information of point cloud into a dynamical filter to modulate the point-wise features. Conditioned on these semantic-modulated features, the point deconvolution block progressively refines point cloud by multi-scale relation learning. Hence, unlike the previous refinement networks [5], [7], [11], our SCR network can effectively alleviate shape confusion among various categories.

Finally, we evaluate our CP3 on the widely-used point cloud completion benchmarks such as MVP [5] and PCN [1]. The extensive experiments show that our IOI pretraining and SCR predicting can effectively boost point cloud generation and refinement. Consequently, CP3 outperforms a number of state-of-the-art approaches with a large margin,

e.g., it achieves the new SOTA result on both MVP and PCN datasets, with 2.27 CD loss on MVP (the current SOTA [5] is 3.06) and 7.02 CD loss on PCN (the current SOTA [7] is 7.21). We will release our code afterwards.

2 RELATED WORK

2.1 3D shape Completion

Most traditional completion methods rely on shape continuity inferred from input scan. Some methods [12], [13], [14], [15], [16] are mainly based on hand-crafted rules or smooth interpolation/extrapolation to characterize the missing regions. Generative based methods [17], [18], [19] is to exploit the large-scale shape database to search for the similar shapes/patches to fill the missing regions of 3D shapes. However, the generalization capability of these methods to diverse partial structures is usually limited. In contrast, deep learning methods can learn more flexible representations for more complicated shapes. The existing deep learning methods are mainly based on the coarse-to-fine style, which generates a coarse one and refines the

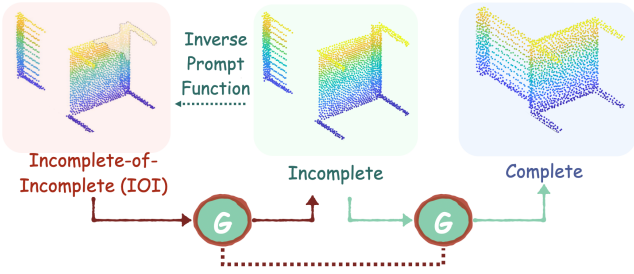


Fig. 2: IOI pretraining and prompting.

geometry details. PCN [1] first operates on raw point clouds and generates a coarse completion based on learned global representation and folding based decoding [20]. Based on PCN, many methods [1], [2], [3], [4] achieve more detailed point cloud completion with better completion results, but usually lack the long-range correlations in local regions. [5], [7], [11] adopt transformers [21] to learn the structural information of pairwise interactions and context correlations. However, they pay much attention to the complicated model structures and usually integrate the generation designs and refinement designs in a single framework, while ignoring deep investigation of distinct data problems in each stage. In addition, a self-supervised approach has been introduced for scene completion with RGB-D scans [22], while different data formulation and task definition make it hard for traditional point cloud completion. Different from the previous approaches, we creatively reinterpret the existing completion process as prompt (generation) and predict (refinement), inspired by the “pretrain-prompt-predict” paradigm in NLP [8]. Moreover, we propose an IOI pretraining for data-diversified generation, and develop a discriminative refinement network with semantic guidance.

2.2 Conditional Feature Modulation

Conditional feature modulation has been used extensively in prior and concurrent works including discrete labels [23], [24], text [25], and images [26]. For example, Condition GAN [23] can generate the controllable images conditioned on class labels. AdaIN [27] can effectively achieve image transfer by matching feature statistics of content and style. StyleGANs [28], [29] design modulations in the generator to adjust the ‘style’ of an image. [30] propose a global feature modulation method for photo retouching. Inspired by these modulation methods, we introduce a semantic-guided modulation for point cloud completion, which can effectively reduce shape confusion for discriminative refinement.

2.3 Prompting Paradigm

Recently, the prompting paradigm has attracted a lot of attention in NLP [8], [31], [32]. The conventional training paradigm refers to pretrain-finetune, while the prompting paradigm is characterized as pretrain-prompt-predict. Specifically, it is used to rebuild the input text through some prompt information, and transfer the predetermined task to the prompting task, e.g., “I love this movie.” is changed into “I love this movie. Overall, it was a __ movie.”. Unlike supervised learning, prompting dose not need to fine tune

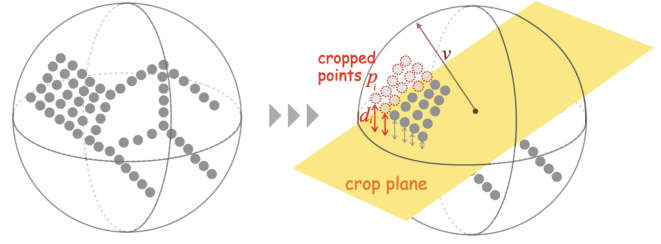


Fig. 3: The crop procedure of IOI sampling.

the whole model, but to design a text prompt to rebuild the model. Specifically, it transfers the knowledge in a large number of pretrained models and rearranges prompting tasks to make them closer to pre-determined tasks. By designing appropriate prompts, a number of works [10], [33], [34] generalizes the model behavior well, so that the pretrained language model can be effectively adapted to predict the desired output in NLP. Moreover, such prompting paradigm has been also introduced for vision-language modeling in computer vision [35]. To our best knowledge, we are the first to leverage such “Pretrain-Prompt-Predict” paradigm for point cloud completion, where we unify point cloud generation and refinement as the prompting and predicting stage, and introduce a self-supervised pretraining stage with the help of our inverse prompt function.

3 METHOD

Overall Paradigm of Our CP3. In this section, we introduce the proposed CP3 paradigm in details. As shown in Fig. 1, we unify point cloud completion by the recent prompting paradigm in NLP. Specifically, point cloud generation refers to the prompting stage. Given an incomplete point cloud (i.e., *prompt*), the generation network is to produce an imperfect completion (i.e., *answer*). Since the training pairs in this stage are predefined with limited data diversity, learning the generation network from scratch leads to unsatisfactory overfitting. To tackle the above problem, we introduce a pretraining stage for point cloud generation. In particular, we design an *inverse prompt function*, i.e., Incompletion-Of-Incompletion (IOI) sampling, which randomly crops incomplete point clouds (i.e., *prompt*) into a large number of diversified IOI point clouds (i.e., *input*). Subsequently, we pretrain the generation network with a self-supervised pretext task, where we use IOI point cloud as input to reconstruct the corresponding incomplete one. Finally, we reinterpret the refinement stage as the predicting stage, where we predict the target point cloud (i.e., *output*) from the imperfect or coarse one (i.e. *answer* in the prompting stage). To enhance such an answer mapping, we introduce a novel Semantic Conditional Refinement (SCR) network. It can effectively reduce shape confusion by progressively refining multi-scale point cloud with its semantic category.

3.1 Pretrain & Prompt: Point Cloud Generation with IOI-Pretrain

As discussed before, we rethink point cloud generation by the prompting stage in NLP, where an incomplete point

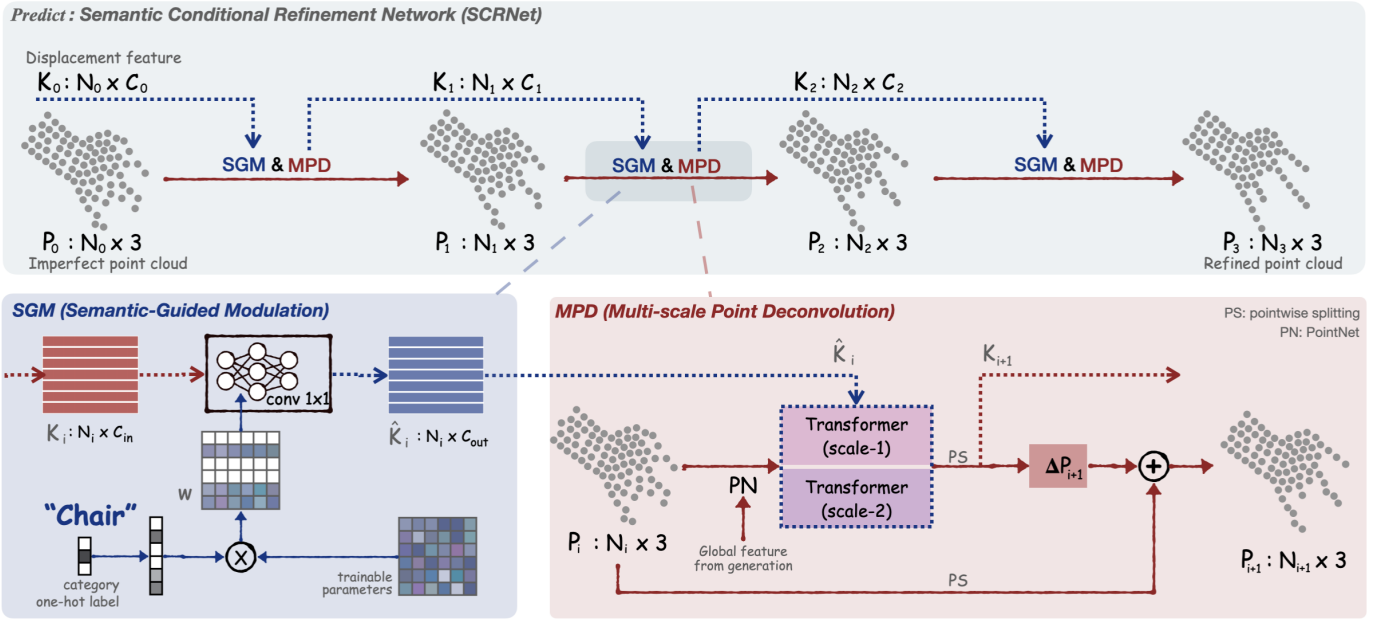


Fig. 4: The structure of SCR network with Semantic-Guided Modulation and Multi-scale Point Deconvolution.

cloud is analogous to an incomplete sentence, e.g., “I love this movie. Overall, it was a __ moive”. But differently, a well-pretrained language model is ready for the prompting stage in NLP, while such a model is not available for point cloud generation. In fact, the existing generation models [1], [4], [5] are trained from scratch, with limited diversity of training pairs. As a result, its performance would be restricted, when tackling new incomplete variations. To enhance its robustness, we propose a self-supervised pre-training stage for the generation model, based on a concise Incompletion-Of-Incompletion (IOI) sampling mechanism.

IOI Sampling as Inverse Prompt Function. To construct the diversified inputs for pretraining, we propose a concise IOI sampling mechanism, which generates incomplete-of-incomplete point clouds (i.e., *input*) from incomplete ones (i.e., *prompt*). We call IOI as *inverse prompt function*, with inspiration of *prompt function* in NLP. The difference is that, the prompt function in NLP is to convert *input* as *prompt* for answer search, while our inverse prompt function is to construct diversified *input* from the given *prompt*. Specifically, the IOI sampling is based on the following procedure in right part of Fig. 3. **First**, we randomly determine a crop plane through the given incomplete point cloud. In particular, a random vector v is ascertained from the object center through two random angle ϕ and θ , where $v = \{\sin(\theta) \cos(\phi), \sin(\theta) \sin(\phi), \cos(\theta)\}$. Then we find the crop plane which is perpendicular to this vector v and passes through the center of point cloud (i.e., yellow plane in Fig. 3). **Second**, we calculate the projection distance d_i from each point p_i to this crop plane,

$$d_i = (p_i - \frac{1}{N} \sum_{j=1}^N p_j) \circ v, \quad (1)$$

where \circ is the hadamard product. **Finally**, we use the projection distance d_i as sampling guidance, and drop the farthest rN points from the crop panel, i.e., red points in Fig.

3. The crop rate is set as $r \in [0, \Gamma]$, where Γ is the maximum threshold. It is worth mentioning that, our IOI sampling brings the following benefits. On one hand, the random crop of incomplete point cloud can generate rich data diversity for pretraining. On the other hand, it naturally builds up a pretext task for self-supervised pretraining as follows.

Self-Supervised Pretraining. By IOI sampling, we have incomplete point clouds and their incomplete-of-incomplete variations on hand. Hence, we can pretrain the generation network by self-supervised learning of incomplete point cloud, i.e., we recover the incomplete point cloud from its IOI point cloud, as shown in Fig. 2. Moreover, we would like to emphasize that, our pretraining task is actually similar to the original generation task (i.e., the prompting stage), by analogy with the “incomplete-to-complete” mapping. Hence, such design can effectively reduce the task gap for model transfer, which perfectly matches the insight of prompting in NLP [8], [31]. Finally, we choose the recent VRCNet [5] as an exemplar of the generation network for pretraining. Note that, other generation networks also work with our pretraining design. More details can be found in Subsection 4.3 and in Table 8.

Prompting. At the generation stage, we are actually given with limited training pairs of incomplete and complete point clouds. Hence, we simply fine-tune the generation network with these pairs, after pretraining. Consequently, we use the well-tuned network for prompting, i.e., generating a coarse complete one (i.e., *answer*) from an incomplete point cloud (i.e., *prompt*).

3.2 Predict: Point Cloud Refinement with Semantic Guidance

After obtaining the coarse point cloud (i.e., *answer*) from the incomplete one (i.e., *prompt*), we next map *answer* into *output*, i.e., the target complete point cloud. As discussed in

the introduction, this predicting stage refers to point cloud refinement. However, the existing refinement networks [4], [6] ignore semantic understanding when recovering the shape of point cloud. This leads to unsatisfactory completion on those confused categories. To tackle this problem, we propose a novel Semantic Conditional Refinement Network (SCRNet), which progressively modulates multi-scale point cloud representation, with guidance of high-level semantics. As shown in Fig. 4, it mainly consists of two core blocks, i.e., Semantic-Guided Modulation (SGM) block and Multi-scale Point Deconvolution (MPD) block. In each refinement unit, the SGM block first adjusts point-wise representation discriminatively, by a dynamic convolution of semantic information. Then, the MPD block further refines the modulated representation of point cloud, by multi-scale aggregation of geometrical context.

Semantic-Guided Modulation (SGM) Block. To reduce shape confusion, we introduce a new Semantic-Guided Modulation (SGM) block, which leverages semantics to modulate point cloud discriminatively. We mainly use the category as the semantic information for illustration. The semantics can be also a learnable global representation of point cloud, as shown in Table 10. For convenience, we omit the subscript i for the i -th refinement unit in the following. As shown in Fig. 4, we introduce a distinct convolution with the semantic-guided filter $\mathbf{W} \in \mathbb{R}^{C_{in} \times C_{out}}$ in the SGM block. We use this convolution to learn the semantic-relevant feature $\hat{\mathcal{K}} \in \mathbb{R}^{N \times C_{out}}$ from the displacement feature $\mathcal{K} \in \mathbb{R}^{N \times C_{in}}$,

$$\hat{\mathcal{K}}(j, q) = \sum_{p=1}^{C_{in}} \mathbf{W}(p, q) \cdot \mathcal{K}(j, p), \quad (2)$$

where j enumerates the number of points N , p enumerates the number of input channels, and q enumerates the number of output channels. Moreover, the displacement feature \mathcal{K} is initialized with the point-wise feature from generation.

More specifically, the semantic-guided filter \mathbf{W} is constructed with the following steps. First, we use the one-hot label vector S of point cloud to construct a category-relevant scale vector $\vartheta(S) \in \mathbb{R}^{C_{in}}$, where $\vartheta(\cdot)$ refers to the MLP layer. Second, we use this scale vector as semantic guidance to generate the filter matrix $\mathbf{B} \in \mathbb{R}^{C_{in} \times C_{out}}$,

$$\mathbf{B}(p, q) = \vartheta(S)_p \cdot \mathbf{A}(p, q), \quad (3)$$

where $\mathbf{A} \in \mathbb{R}^{C_{in} \times C_{out}}$ is a trainable parameter matrix. By this operation, $\vartheta(S)_p$ can modulate the p -th feature channel of input point cloud. Finally, we normalize the filter matrix for optimization stability,

$$\mathbf{W}(p, q) = \mathbf{B}(p, q) / \sqrt{\sum_{p=1}^{C_{in}} \mathbf{B}(p, q)^2 + \epsilon}, \quad (4)$$

where ϵ is a small constant to avoid numerical issues. Based on this normalized filter \mathbf{W} , we can modulate different feature channels according to semantic category. As a result, our SGM block makes the refinement stage more discriminative, which can effectively distinguish point clouds that have similar local shapes but belong to different categories. **Multi-scale Point Deconvolution (MPD) Block.** After obtaining the modulated feature, we use it for point cloud refinement. As shown in Fig. 4, we choose snowflake point

deconvolution [7] as our base operation, which learns the point displacement progressively to refine the shape. For the i -th block, it firstly constructs the input feature \mathcal{Q}_i , by concatenating the predicted point cloud \mathcal{P}_i with its global feature from PointNet [36]. Second, it sends \mathcal{Q}_i and $\hat{\mathcal{K}}_i$ into the skip transformers [7] for point relation learning, where $\hat{\mathcal{K}}_i$ is the modulated displacement feature from the previous block. The output of skip transformers is denoted as \mathcal{H}_i . Third, it upsamples \mathcal{H}_i as displacement feature \mathcal{K}_{i+1} for next layer and generates the coordinate variation $\Delta\mathcal{P}_{i+1}$ in the current block, by point-wise splitting operation in [7]. Finally, it adds the coordinate variation $\Delta\mathcal{P}_{i+1}$ with the duplicated previously-predicted point cloud \mathcal{P}_i , which generates the refined point cloud \mathcal{P}_{i+1} in the current block.

Note that, our MPD block follows the refinement style of snowflake point deconvolution. But differently, it is equipped with our semantic-guided modulation block and multi-scale relation learning. First, we use the modulated feature $\hat{\mathcal{K}}_i$ of SGM block as input to skip transformer, instead of using the original displacement feature \mathcal{K}_i . In this way, we flexibly integrate semantic category information into relation learning, which enhances the shape-context feature \mathcal{H}_i for discriminative refinement. Second, we introduce multi-scale learning strategy for skip transformers, instead of building point relations in a single scale. For example, we use skip transformers with two different local regions to learn shape context features \mathcal{H}_i^1 and \mathcal{H}_i^2 . Next, we fuse these context features to obtain the displacement feature \mathcal{K}_{i+1} in the current block,

$$\mathcal{K}_{i+1} = \text{MLP}(\varphi(\mathcal{H}_i^1 \oplus \mathcal{H}_i^2)) \quad (5)$$

where \oplus is the concatenation operation, and φ is the point-wise splitting operation [7] for upsampling. Via such multi-scale design, our MPD block can effectively capture complicated shape variations in the point clouds.

4 EXPERIMENTS

4.1 Implementation Details

In this subsection, we will introduce the specific implementation details of pretrain, prompt and predict in our CP3 paradigm, as well as the training details of the whole framework. Firstly, we use inverse prompt function to construct the pretraining pairs, where the threshold Γ of IOI pretraining is set to 0.9. Then we pretrain the generation network in the self-supervised way. After training the generation stage, we fix it to extract the global feature and point-wise feature of the last layer, and feed them to train the refinement stage. In semantic-guided predict stage, we use three blocks to recover the local details iteratively, based on the imperfect point cloud from prompt stage, as shown in Fig. 4. For various resolutions of datasets, we can adjust the upsampling multiplier in the MPD block to upsample at different scales in training, e.g., for 2,048 points of imperfect point cloud and 16,384 points of target point cloud, we can set the multipliers of three MPD blocks to [1, 1, 8] and choose local regions of multi-scale transformer with 12 and 24. The loss functions of generation stage is the KL divergence loss [5] and CD loss, the refinement loss function is CD loss.

For training details, the batch size is set to 64. The optimizer is Adam optimizer with initial learning rate 1×10^{-4}

Method	airp.	cabinet	car	chair	lamp	sofa	table	waterc.	bed	bench	books.	bus	guitar	motor.	pistol	skateb.	Avg.
PCN [1]	2.95	4.13	3.04	7.07	14.93	5.56	7.06	6.08	12.72	5.73	6.91	2.46	1.02	3.53	3.28	2.99	6.02
TopNet [37]	2.72	4.25	3.40	7.95	17.01	6.04	7.42	6.04	11.60	5.62	8.22	2.37	1.33	3.90	3.97	2.09	6.36
MSN [3]	2.07	3.82	2.76	6.21	12.72	4.74	5.32	4.80	9.93	3.89	5.85	2.12	0.69	2.48	2.91	1.58	4.90
Wang et. al. [2]	1.59	3.64	2.60	5.24	9.02	4.42	5.45	4.26	9.56	3.67	5.34	2.23	0.79	2.23	2.86	2.13	4.30
ECG [4]	1.41	3.44	2.36	4.58	6.95	3.81	4.27	3.38	7.46	3.10	4.82	1.99	0.59	2.05	2.31	1.66	3.58
GRNet [6]	1.61	4.66	3.10	4.72	5.66	4.61	4.85	3.53	7.82	2.96	4.58	2.97	1.28	2.24	2.11	1.61	3.87
NSFA [38]	1.51	4.24	2.75	4.68	6.04	4.29	4.84	3.02	7.93	3.87	5.99	2.21	0.78	1.73	2.04	2.14	3.77
SnowFlakeNet [7]	1.16	3.32	2.41	2.97	5.46	3.58	3.82	2.72	6.72	2.80	4.10	1.80	0.52	1.90	1.82	2.70	3.18
VRCNet [5]	1.15	3.20	2.14	3.58	5.57	3.58	4.17	2.47	6.90	2.76	3.45	1.78	0.59	1.52	1.83	1.57	3.06
Ours	0.74	2.94	2.25	2.78	2.54	2.87	2.84	2.00	5.24	1.98	2.87	1.67	0.45	1.45	1.23	0.92	2.27

TABLE 1: Completion results (L2 Chamfer distance $\times 10^4$) on MVP dataset (16,384 points).

Method	airp.	cabinet	car	chair	lamp	sofa	table	waterc.	bed	bench	books.	bus	guitar	motor.	pistol	skateb.	Avg.
PCN [1]	0.82	0.61	0.69	0.52	0.46	0.55	0.65	0.63	0.45	0.69	0.55	0.78	0.91	0.67	0.77	0.86	0.638
TopNet [37]	0.79	0.62	0.61	0.44	0.39	0.51	0.64	0.61	0.41	0.68	0.52	0.77	0.87	0.62	0.73	0.84	0.601
MSN [3]	0.88	0.69	0.69	0.60	0.60	0.63	0.73	0.80	0.57	0.80	0.64	0.81	0.94	0.73	0.81	0.89	0.710
Wang et. al. [2]	0.90	0.69	0.73	0.67	0.68	0.64	0.75	0.74	0.60	0.80	0.66	0.80	0.93	0.77	0.84	0.90	0.740
ECG [4]	0.91	0.68	0.72	0.68	0.73	0.65	0.77	0.75	0.64	0.82	0.71	0.80	0.95	0.78	0.84	0.90	0.753
GRNet [6]	0.85	0.58	0.65	0.64	0.71	0.58	0.69	0.72	0.59	0.77	0.64	0.68	0.87	0.74	0.79	0.85	0.692
NSFA [38]	0.90	0.69	0.72	0.74	0.78	0.71	0.82	0.80	0.69	0.85	0.75	0.82	0.93	0.82	0.86	0.89	0.783
SnowFlakeNet [7]	0.92	0.70	0.73	0.72	0.78	0.70	0.80	0.79	0.68	0.85	0.73	0.82	0.95	0.80	0.87	0.92	0.782
VRCNet [5]	0.93	0.72	0.76	0.74	0.79	0.70	0.81	0.80	0.65	0.86	0.76	0.83	0.96	0.83	0.89	0.93	0.796
Ours	0.94	0.74	0.75	0.77	0.84	0.74	0.82	0.82	0.72	0.87	0.77	0.84	0.97	0.85	0.90	0.93	0.814

TABLE 2: Point cloud completion results (F-Score@ 1%, higher is better) on MVP dataset (16,384 points).

# Points	2,048		4,096		8,192		16,384	
	CD	F1	CD	F1	CD	F1	CD	F1
PCN [1]	9.77	0.320	7.96	0.458	6.99	0.563	6.02	0.638
TopNet [37]	10.11	0.308	8.20	0.440	7.00	0.533	6.36	0.601
MSN [3]	7.90	0.432	6.17	0.585	5.42	0.659	4.90	0.710
Wang et. al. [2]	7.25	0.434	5.83	0.569	4.90	0.680	4.30	0.740
ECG [4]	6.64	0.476	5.41	0.585	4.18	0.690	3.58	0.753
VRCNet [5]	5.96	0.499	4.70	0.636	3.64	0.727	3.06	0.796
SnowFlakeNet [7]	6.05	0.500	4.77	0.651	3.80	0.747	3.18	0.782
Ours	5.10	0.526	3.49	0.682	3.14	0.756	2.27	0.814

TABLE 3: Comparisons on MVP dataset with various resolutions.

(decayed by 0.7 every 40 epochs). For the environment, our framework is implemented by PyTorch 1.5 and RTX 8000 GPUs (each with 48 GB memory consumption). As for resource usage, our modulation module contains only less than 43k parameters. The model parameters / inference time of our SCRNet is 20.7M / 0.52s, PoinTr [11] is 30.9M / 0.65s, SnowFlakeNet [7] is 19.2M / 0.61s, but we have the best completion result (as Table 3 and 4 shows).

4.2 Comparison with State-Of-The-Art

Evaluation on MVP Dataset. The MVP dataset is generated by CAD models selected from ShapeNet [39]. Compared with other datasets [1], [37], the MVP dataset is more challenging in incomplete variations (partial point clouds rendered from 26 views) and rich categories (16 categories). In order to accurately evaluate the quality of the completions at different resolutions, it also provides complete point clouds with different resolutions, including 2048 (1x), 4096 (2x), 8192 (4x) and 16384 (8x). For evaluation, we follow the same metrics with VRCNet [5] to fairly compare our method with other methods, where L2 version of Chamfer Distance

(CD) [37] is used to evaluate average closest point distance and align with previous studies, and F-score [40] evaluates the distance between object surfaces, which is defined as the harmonic mean between precision and recall. The evaluated CD and F-score for all evaluated methods (16,384 points) are reported in Table 1 and 2, respectively. Additionally, we re-implemented the official code of SnowFlakeNet [7] for fair comparison. We can find that our method can achieve the best performance in CD loss with 2.27 and F-score @ 1% with 0.814. We compare our methods with existing methods that support multi-resolution completion in Table 3. Our method outperforms all the other methods with a large margin.

Evaluation on PCN Dataset. The widely-used PCN [1] dataset is a subset of the ShapeNet dataset [39] with 8 categories. The incomplete shapes are generated by back-projecting complete shapes into 8 different partial views. For each complete shape, 16,384 points are evenly sampled from the shape surface. For fair comparison, we adopt the L1 version of chamfer distance as the evaluation metric, which follows the same practice as previous methods [1], [7], [11]. The results are summarized in Table 4, our method can achieve 7.02 performance and outperform other state-of-the-art methods in most categories.

Qualitative Analysis of different methods. To make comparisons under the challenging situations, we visualize the completion results of different methods on MVP dataset with 16,384 points. The qualitative results are shown in Fig. 5. Compared to other methods, our proposed CP3 can recover better complete shapes with fine details. Our method largely improves completion for confused classes (e.g., table & chair). Especially for objects with challenging partial areas and complex geometry, our method can achieve the precise and reasonable completion, e.g., for the lamp

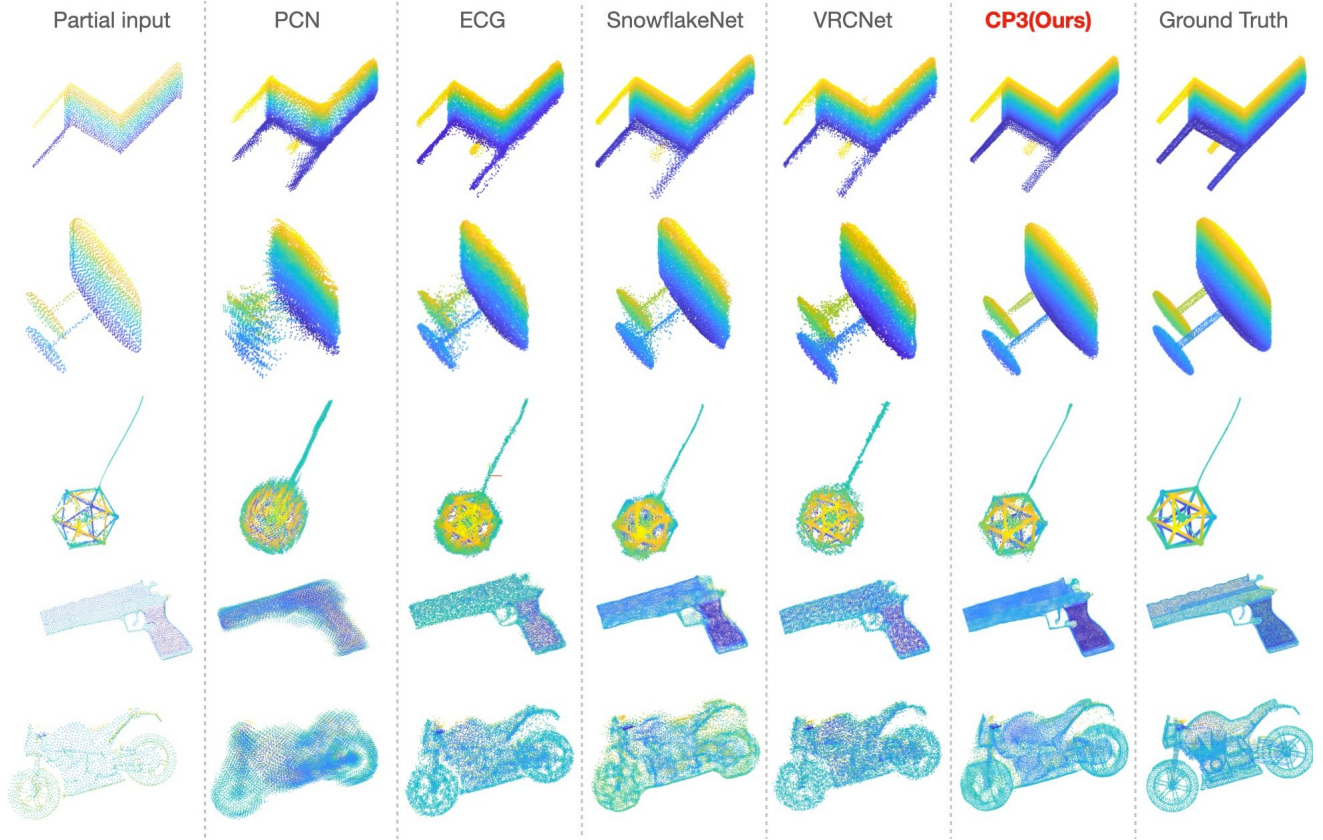


Fig. 5: Qualitative completion results on the MVP dataset by different methods.

Methods	Plane	Cabinet	Car	Chair	Lamp	Couch	Table	Boat	Avg.
FoldingNet [20]	9.49	15.80	12.61	15.55	16.41	15.97	13.65	14.99	14.31
TopNet [37]	7.61	13.31	10.90	13.82	14.44	14.78	11.22	11.12	12.15
AtlasNet [41]	6.37	11.94	10.10	12.06	12.37	12.99	10.33	10.61	10.85
PCN [1]	5.50	22.70	10.63	8.70	11.00	11.34	11.68	8.59	9.64
GRNet [6]	6.45	10.37	9.45	9.41	7.96	10.51	8.44	8.04	8.83
CDN [2]	4.79	9.97	8.31	9.49	8.94	10.69	7.81	8.05	8.51
PMP-Net [42]	5.65	11.24	9.64	9.51	6.95	10.83	8.72	7.25	8.73
NSFA [38]	4.76	10.18	8.63	8.53	7.03	10.53	7.35	7.48	8.06
PoinTr [11]	4.75	10.47	8.68	9.39	7.75	10.93	7.78	7.29	8.38
SCRN [43]	4.80	9.94	9.31	8.78	8.66	9.38	7.20	7.91	8.29
SnowflakeNet [7]	4.29	9.16	8.08	7.89	6.07	9.23	6.55	6.40	7.21
Ours	4.34	9.02	7.90	7.41	6.35	8.52	6.32	6.26	7.02

TABLE 4: Comparisons on PCN dataset (L1 Chamfer distance $\times 10^3$).

with fine geometric details, we recover the details to the greatest extent. For the pistol and motorbike with large partial areas, our completions are not only detailed, but also has less noise and a more uniform local density, we can see that there is less noise at the trigger and motor tires.

4.3 Analysis

4.3.1 Ablation Studies of Overall Framework

In order to examine the effectiveness of our designs, we conducted detailed ablation studies based on our framework for MVP dataset (2048 points). The results are summarized in Table 5. (i) only has the generation stage (prompt), where the result is 5.96. Based on the prompt, (ii) adds the predict stage to point cloud refinement. The result improves to 5.80 due to our semantic modulation strategy

for discriminative shape recovery. (iii) and (iv) add the IOI pretraining paradigm. When the completion model only includes the generation stage, the result is improved to 5.69. While we use the entire framework of CP3, the result can be improved to 5.10. It can be concluded that our proposed IOI pretraining and semantic-guided refinement can greatly improve the performance of point cloud completion.

To qualitatively validate our framework, we conduct a visual comparison of some of the models in Table 5. The results are shown in Figure 6. We can clearly observe that complete results of *i* (baseline) have some defects, e.g., the density of incomplete area and complete area is inconsistent, noise points will be generated in the hollowed out area and some missing regions can not be complete enough. With the IOI pretrain *iii*, the large missing area can be more complete. e.g., compared with setting *i*, the incomplete area

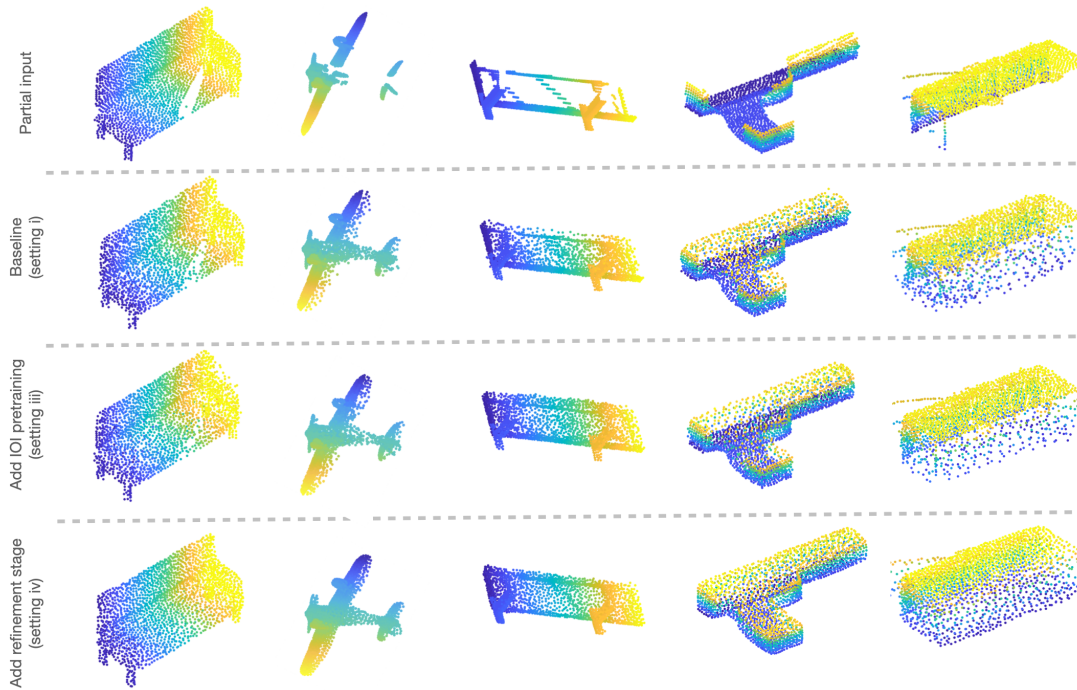


Fig. 6: Qualitative completion results (2,048 points) by different ablation settings.

CP3	Pretrain (IOI)	Prompt	Predict	CD
<i>i</i>	×	✓	×	5.96
<i>ii</i>	×	✓	✓	5.80
<i>iii</i>	✓	✓	×	5.69
<i>iv</i>	✓	✓	✓	5.10

TABLE 5: Ablation studies of the CP3 framework on MVP dataset with 2048 points (CD multiplied by 10^4), “✓” means that we use the corresponding strategies, while “×” means that the relevant strategies is not applicable.

	Pretraining input	Pretraining Target	CD
Pre-1	Mirrored Incompletion	Completion	7.59
Pre-2	Jittered Incompletion	Completion	7.16
Pre-3	Incompletion	Completion	5.96
Pre-4	Incompletion	Incompletion	5.78
Pre-5	Incompletion-of-Incompletion	Completion	6.03
Pre-6	hybrid training as SCRNN [43]		5.75
Pre-7	Incompletion-of-Incompletion	Incompletion	5.69

TABLE 6: Ablation studies of IOI pretraining: different pretraining settings.

of the bench is more complete in setting *iii*. When adding the semantic conditional network for refinement (setting *iv*), the density problem can be solved effectively and the missing areas can be more complete.

4.3.2 Ablation Studies of IOI Pretraining

Why does the IOI pretraining work? To verify the effectiveness of our IOI pretraining, we compare a variety of pretraining pairs in Table 6. When we use the incompletion to reconstruct itself (“Pre-4”), the result can improve to 5.78, because the model learns the distribution of each incomplete point cloud independently, and then plays a better generalization in the generation stage. Next we try to use comple-

threshold Γ	0.1	0.3	0.5	0.7	0.9
CD	5.80	5.78	5.73	5.71	5.69

TABLE 7: Ablation studies of IOI pretraining: different maximum threshold of the crop rate.

Generation Network	w/o IOI Pre.	w IOI Pre.
PCN [1]	9.77	8.51
ECG [4]	6.64	6.34
VRCNet [5]	5.96	5.69

TABLE 8: Ablation studies of IOI pretraining: different generation networks.

tion as a pretext task (“Pre-5” and “Pre-7”). Compared with incomplete point cloud, the incomplete of incomplete point cloud has a greater degree and more diverse partial areas, because it has undergone the twice incomplete treatment. It is difficult for the network to complete the IOI input to the complete target. Therefore, it is more appropriate to process the augmented input to the original incomplete point cloud. As we can see, “Pre-5” is 6.03, while “Pre-7” improves to 5.69. We also consider some commonly used data diversified operations in point cloud, e.g., mirroring and jittering the point cloud, demonstrating by the “Pre-1” and “Pre-2”. As for comparison with other pretraining method for generation stage, we used the same pretraining strategy as SCRNN [43]. SCRNN is a hybrid training of shape completion (“IOI” to “I”) and partial reconstruction (“IOI” to “IOI”) in a *parallel* manner. Such pretraining may mislead the model, by using the similar input but with different supervision. In contrast, our CP3 follows a *serial* training manner from NLP, with “IOI” to “I” for pretraining and then “I” to “C” for prompting. To show our effectiveness, we conduct such parallel style of SCRNN as “Pre-6”. The

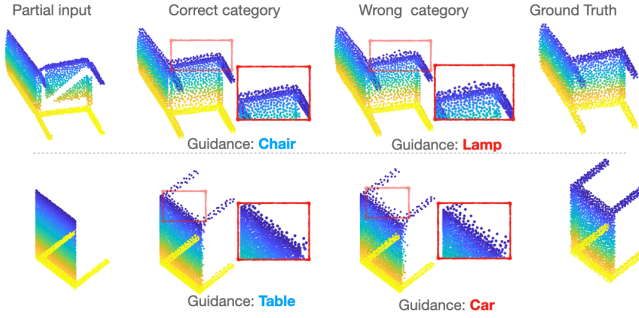


Fig. 7: Evaluating with wrong category guidance. Left: Qualitative evaluation results of different setting to the category guidance. Right: Comparisons of correct/wrong category guidance for evaluation on MVP dataset (*Lower is better*).

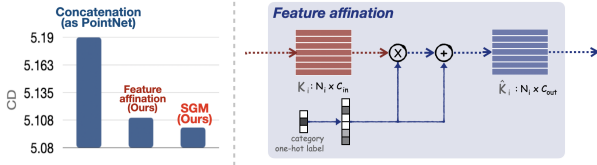
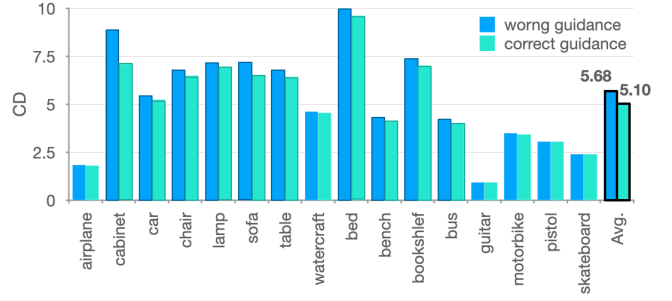


Fig. 8: Left: Comparisons of different semantic guidance operation. Right: Details of feature affination.

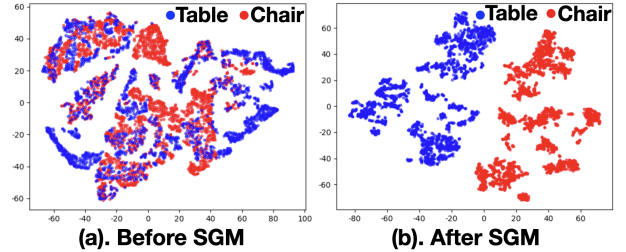


Fig. 9: TSNE visualization of features before and after semantic guided modulation.

CD loss ($\times 10^4$) of parallel manner is worse (parallel vs our serial: 5.75 vs 5.69). In addition, based on “Pre-7”, we also compare the maximum threshold Γ of the crop rate based on the IOI pretraining, which is shown in Table 7. Through the series of experiments, we finally determine the threshold Γ is 0.9.

Can IOI pretrain paradigm work for other networks?

Here we compare the effectiveness of IOI pretraining for different networks (e.g., PCN [1], ECG [4] and VRCNet [5]) in Table 8. With IOI pretraining, the performance of such mainstream completion networks is greatly improved in varying degrees. It can be concluded that the IOI pretraining is a general and effective new training paradigm for point cloud completion task.

4.3.3 Ablation Studies of Semantic Refinement

Why does the semantic refinement work? To validate the designs of our predict (semantic-guided refinement) stage, we first conduct three different variations as Table 9 shows. When we use the basic refinement network without semantic-guided modulation and multi-scale transformer strategy, the result is 5.60. With the semantic modulation, the charmer distance reduces to 5.17. Subsequently, when adding the multi-scale strategy in the MPD blocks, the final result can achieve to 5.10. Moreover, we investigate different conditional information in Table 10. It can be concluded from the experiments that under the modulation of category semantics and global learnable semantic, the performance can be greatly improved. Specially, the category semantics is more effective as the conditional information. In order to further validate Semantic-Guided Modulation (SGM) block, we conduct a series of comparative experiments of whether to use the SGM block in each layer of our SCRNet, which

is shown in Table 11. It is relatively more efficient to use semantic-guided modulation blocks at the front layers. Moreover, for the multi-scale strategy, we conduct different settings for the transformer scale in Table 12, which indicates that it is more effective to choose a larger local pattern of fusion.

Why semantic label contributes to completion task? Analysis from the perspective of point-wise representation, our SGM modulate seach point-wise feature with semantic label. This can effectively distinguish point clouds which have similar local details but belong to different categories. In Fig. 9, we show point-wise feature distribution of two point clouds (chair and table), Clearly, the point-wise features of two point clouds (chair and table) are distinguished after using our SGM.

Evaluating with wrong category guidance. To verify the effectiveness of semantic-guided modulation on different categories, we use model *iv* in Table 5 to evaluate our CP3 with different strategies of category guidance. The results are shown in Fig. 7. When we randomly replace the categories of all test point clouds, and the CD loss becomes larger (i.e., 5.68). For further analysis, we show the test results for all categories. We can see that, for a small number of categories with high discrimination (e.g., airplane, watercraft, guitar), their completions are not greatly affected by the wrong guidance. While for most confusing categories with similar structures, such as chair sofa and table, the evaluation results are heavily deteriorated by the wrong guidance. The visualization of chair and table in Fig. 7 can also verify this viewpoint. The local area will have more

Semantic modulation	Multiscale operation	CD
×	×	5.60
✓	×	5.17
✓	✓	5.10

TABLE 9: Ablation studies of our SCRNet for refinement: SGM and MPD blocks in the refinement.

Conditional information	CD
Without semantics	5.60
Category semantics	5.17
Global learnable semantics	5.25
Category + Global learnable semantics	5.22

TABLE 10: Ablation studies of our SCRNet for refinement: conditional information in our semantic-guided modulation.

noise points under the wrong guidance than the correct category guidance. It shows that our semantic conditional modulation network is effective to reduce shape confusion.

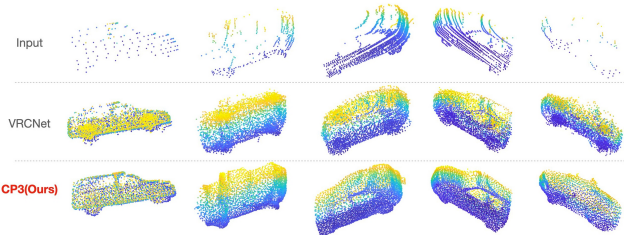


Fig. 10: Qualitative results on the KITTI dataset. Our method generates more complete and locally detailed shapes for the real scanned cars.

Comparison with other semantic guidance operations.

Here we investigate different operations for feature modulation. In addition to our semantic guided modulation, we also try concatenation and feature affination which inspired by [30], [44]. As Figure 8 (right) shows, feature affination aims at scaling and shifting the intermediate features \mathcal{K} by the semantic information. This operation can be formulated as: $\hat{\mathcal{K}} = \sigma(\mathcal{K}) \odot \alpha + \beta$, where \odot denotes the element-wise multiplication operation and σ is MLP layers, $\mathcal{K} \in \mathbb{R}^{N \times C}$ is the intermediate displacement features from MPD block, $\alpha, \beta \in \mathbb{R}^{1 \times C}$ are affine parameters that are estimated from the point cloud category labels $S \in \mathbb{R}^{1 \times C_{cate}}$ via MLP layers. We use conditional vector α to affect the cluster centers of the local representation and use conditional vector β to fine-tune the variance in the feature space. Thus, we can achieve point feature global adjustment with only few parameters. The comparisons of different modulate operations are reported in Fig. 8 (left). From the looks of it, PointNet [36] simply concatenates the category and point-wise features, which ignores the discriminative interaction between them. Alternatively, our SGM converts category into a dynamical filter to modulate all the point-wise features with semantic information. Our semantic guided modulation and feature affination provide a performance boost. Therefore, the model is not easy to be confused with the similar local structures of different semantic information.

1-st layer	2-nd layer	3-rd layer	CD
✓	×	×	5.17
×	✓	×	5.18
×	×	✓	5.20

TABLE 11: Ablation studies of our SCRNet for refinement: whether to use the semantic-guided modulation block in each layer.

Strategy	local regions (k)	CD
single-scale	[12]	5.17
multi-scale	[12, 24]	5.10
multi-scale	[6,12]	5.23

TABLE 12: Ablation studies of our SCRNet for refinement: k -nearest neighbours of the multi-scale strategy.

4.3.4 Generalization Analysis to novel unseen categories

To verify the generalization ability to novel unseen categories, following the the setting of [11], we take the first 8 categories of MVP [5] for training and the rest 8 categories of the test data for evaluation. As shown in Table 13, we compare our method with some sota methods, e.g., PointTr [11], VRCNet [5], SnowFlakeNet [7]. Under such challenging situation, our method can achieve the best performance of 7.64. While VRCNet only achieves 9.08 and SnowFlakeNet achieves 8.25.

4.3.5 Completion on real-world Kitti dataset

In order to validate the performance of our CP3 in real-world scenarios, we fine tune our model on ShapeNet-car dataset and test on KITTI-cars [45], following [1], [5]. To show the performance of our CP3 in real-world KITTI-cars dataset, we report the Fidelity error and Consistency in Table 14. Fidelity is calculated from the average distance from each point in the partial input to its nearest neighbour in the output. This measures how well the input is preserved. Consistency is calculated from the average CD distance between the outputs of the same object in successive frames. More details on the evaluation metrics can be found in [1], [6]. Compared to other methods, our CP3 has better consistency between the two consecutive frames and better fidelity error. Moreover, we also show the qualitative visualization results are shown in Fig. 10, our results are more complete overall and less noisy locally. The bodywork of the car has also been refined in detail.

5 CONCLUSION

In this paper, we creatively propose a new paradigm called CP3 for point cloud completion, including IOI pretraining, prompting (generation) and predicting (refinement). IOI pretraining boosts the robustness of generation network by learning a pretext task internally in a self-supervised way. Moreover, we design a novel semantic conditional modulation for point cloud refinement, which uses semantic information as guidance to adaptively modulate point cloud representation for discriminative recovery. Extensive experimental results and visualizations validate the effectiveness of our approach.

Broader Impact. The core of our CP3 is a generic training paradigm, inspired by the well-established natural language

Method	CD
PCN [1]	16.56
ECG [4]	15.23
PoinTr [11]	10.31
VRCNet [5]	9.08
SnowFlakeNet [7]	8.25
Ours	7.64

TABLE 13: Generalization to novel unseen categories on MVP dataset.

	PCN [1]	FoldingNet [20]	NSFA [38]	TopNet [37]	GRNet [6]	Ours
Consistency ↓	1.56	1.05	-	0.57	0.31	0.29
Fidelity error ↓	0.034	0.036	0.026	0.031	-	0.013

TABLE 14: Quantitative comparisons on KITTI dataset.

processing. Hence, it would be interesting to extend this paradigm for other 3D tasks like point cloud scene understanding. Furthermore, it is worth investigating whether it is an effective method for traditional vision tasks like image inpainting. Hopefully, such paradigm can leverage benefits from both CV and NLP for better representation learning in a unified manner.

REFERENCES

- [1] W. Yuan, T. Khot, D. Held, C. Mertz, and M. Hebert, "Pcn: Point completion network," in *3DV*, 2018.
- [2] X. Wang, M. H. Ang Jr, and G. H. Lee, "Cascaded refinement network for point cloud completion," in *Proceedings of the IEEE/CVF conference on computer vision and pattern recognition*, 2020.
- [3] M. Liu, L. Sheng, S. Yang, J. Shao, and S.-M. Hu, "Morphing and sampling network for dense point cloud completion," in *Proceedings of the AAAI conference on artificial intelligence*, 2020.
- [4] L. Pan, "Ecg: Edge-aware point cloud completion with graph convolution," *IEEE Robotics and Automation Letters*, 2020.
- [5] L. Pan, X. Chen, Z. Cai, J. Zhang, H. Zhao, S. Yi, and Z. Liu, "Variational relational point completion network," in *Proceedings of the IEEE/CVF conference on computer vision and pattern recognition*, 2021.
- [6] H. Xie, H. Yao, S. Zhou, J. Mao, S. Zhang, and W. Sun, "Grnet: Griding residual network for dense point cloud completion," in *European Conference on Computer Vision*, 2020.
- [7] P. Xiang, X. Wen, Y.-S. Liu, Y.-P. Cao, P. Wan, W. Zheng, and Z. Han, "Snowflakenet: Point cloud completion by snowflake point deconvolution with skip-transformer," *arXiv preprint arXiv:2108.04444*, 2021.
- [8] P. Liu, W. Yuan, J. Fu, Z. Jiang, H. Hayashi, and G. Neubig, "Pre-train, prompt, and predict: A systematic survey of prompting methods in natural language processing," *arXiv preprint arXiv:2107.13586*, 2021.
- [9] J. Wei, M. Bosma, V. Y. Zhao, K. Guu, A. W. Yu, B. Lester, N. Du, A. M. Dai, and Q. V. Le, "Finetuned language models are zero-shot learners," *arXiv preprint arXiv:2109.01652*, 2021.
- [10] T. Brown, B. Mann, N. Ryder, M. Subbiah, J. D. Kaplan, P. Dhariwal, A. Neelakantan, P. Shyam, G. Sastry, A. Askell *et al.*, "Language models are few-shot learners," *Advances in neural information processing systems*, 2020.
- [11] X. Yu, Y. Rao, Z. Wang, Z. Liu, J. Lu, and J. Zhou, "Pointr: Diverse point cloud completion with geometry-aware transformers," in *Proceedings of the IEEE international conference on computer vision*, 2021.
- [12] S. Shalom, A. Shamir, H. Zhang, and D. Cohen-Or, "Cone carving for surface reconstruction," in *ACM SIGGRAPH Asia*, 2010.
- [13] M. Attene, "A lightweight approach to repairing digitized polygon meshes," *The visual computer*, 2010.
- [14] J. Lin, X. Jin, and C. C. Wang, "Fusion of disconnected mesh components with branching shapes," *The Visual Computer*, 2010.
- [15] W. Hu, Z. Fu, and Z. Guo, "Local frequency interpretation and non-local self-similarity on graph for point cloud inpainting," *IEEE Transactions on Image Processing*, 2019.
- [16] D. T. Nguyen, B.-S. Hua, K. Tran, Q.-H. Pham, and S.-K. Yeung, "A field model for repairing 3d shapes," in *Proceedings of the IEEE/CVF conference on computer vision and pattern recognition*, 2016.
- [17] C.-H. Shen, H. Fu, K. Chen, and S.-M. Hu, "Structure recovery by part assembly," *ACM Transactions on Graphics (TOG)*, 2012.
- [18] T. Shao, W. Xu, K. Zhou, J. Wang, D. Li, and B. Guo, "An interactive approach to semantic modeling of indoor scenes with an rgbd camera," *ACM Transactions on Graphics (TOG)*, 2012.
- [19] A. Martinovic and L. Van Gool, "Bayesian grammar learning for inverse procedural modeling," in *Proceedings of the IEEE/CVF conference on computer vision and pattern recognition*, 2013.
- [20] Y. Yang, C. Feng, Y. Shen, and D. Tian, "Foldingnet: Point cloud auto-encoder via deep grid deformation," in *Proceedings of the IEEE/CVF conference on computer vision and pattern recognition*, 2018.
- [21] A. Vaswani, N. Shazeer, N. Parmar, J. Uszkoreit, L. Jones, A. N. Gomez, Ł. Kaiser, and I. Polosukhin, "Attention is all you need," in *Advances in neural information processing systems*, 2017.
- [22] A. Dai, C. Diller, and M. Nießner, "Sg-nn: Sparse generative neural networks for self-supervised scene completion of rgb-d scans," in *Proceedings of the IEEE/CVF conference on computer vision and pattern recognition*, 2020.
- [23] M. Mirza and S. Osindero, "Conditional generative adversarial nets," *arXiv preprint arXiv:1411.1784*, 2014.
- [24] I. Goodfellow, J. Pouget-Abadie, M. Mirza, B. Xu, D. Warde-Farley, S. Ozair, A. Courville, and Y. Bengio, "Generative adversarial nets," *Advances in neural information processing systems*, 2014.
- [25] S. Reed, Z. Akata, X. Yan, L. Logeswaran, B. Schiele, and H. Lee, "Generative adversarial text to image synthesis," in *ICML*, 2016.
- [26] P. Isola, J.-Y. Zhu, T. Zhou, and A. A. Efros, "Image-to-image translation with conditional adversarial networks," in *Proceedings of the IEEE/CVF conference on computer vision and pattern recognition*, 2017.
- [27] X. Huang and S. Belongie, "Arbitrary style transfer in real-time with adaptive instance normalization," in *Proceedings of the IEEE international conference on computer vision*, 2017.
- [28] T. Karras, S. Laine, and T. Aila, "A style-based generator architecture for generative adversarial networks," in *Proceedings of the IEEE/CVF conference on computer vision and pattern recognition*, 2019.
- [29] T. Karras, S. Laine, M. Aittala, J. Hellsten, J. Lehtinen, and T. Aila, "Analyzing and improving the image quality of stylegan," in *Proceedings of the IEEE/CVF conference on computer vision and pattern recognition*, 2020.
- [30] J. He, Y. Liu, Y. Qiao, and C. Dong, "Conditional sequential modulation for efficient global image retouching," in *European Conference on Computer Vision*, 2020.
- [31] B. Lester, R. Al-Rfou, and N. Constant, "The power of scale for parameter-efficient prompt tuning," *arXiv preprint arXiv:2104.08691*, 2021.
- [32] Y. Lu, M. Bartolo, A. Moore, S. Riedel, and P. Stenetorp, "Fantastically ordered prompts and where to find them: Overcoming few-shot prompt order sensitivity," *arXiv preprint arXiv:2104.08786*, 2021.
- [33] A. Radford, J. Wu, R. Child, D. Luan, D. Amodei, I. Sutskever *et al.*, "Language models are unsupervised multitask learners," *OpenAI blog*, 2019.
- [34] F. Petroni, T. Rocktäschel, P. Lewis, A. Bakhtin, Y. Wu, A. H. Miller, and S. Riedel, "Language models as knowledge bases?" *arXiv preprint arXiv:1909.01066*, 2019.
- [35] K. Zhou, J. Yang, C. C. Loy, and Z. Liu, "Learning to prompt for vision-language models," *arXiv preprint arXiv:2109.01134*, 2021.
- [36] C. R. Qi, H. Su, K. Mo, and L. J. Guibas, "Pointnet: Deep learning on point sets for 3d classification and segmentation," in *Proceedings of the IEEE/CVF conference on computer vision and pattern recognition*, 2017.
- [37] L. P. Tchapmi, V. Kosaraju, H. Rezatofighi, I. Reid, and S. Savarese, "Topnet: Structural point cloud decoder," in *Proceedings of the IEEE/CVF conference on computer vision and pattern recognition*, 2019.
- [38] W. Zhang, Q. Yan, and C. Xiao, "Detail preserved point cloud completion via separated feature aggregation," in *European Conference on Computer Vision*, 2020.
- [39] Z. Wu, S. Song, A. Khosla, F. Yu, L. Zhang, X. Tang, and J. Xiao, "3d shapenets: A deep representation for volumetric shapes," in *Proceedings of the IEEE/CVF conference on computer vision and pattern recognition*, 2015.
- [40] A. Knapitsch, J. Park, Q.-Y. Zhou, and V. Koltun, "Tanks and temples: Benchmarking large-scale scene reconstruction," *ACM Transactions on Graphics (TOG)*, 2017.

- [41] T. Groueix, M. Fisher, V. G. Kim, B. C. Russell, and M. Aubry, "A papier-mâché approach to learning 3d surface generation," in *Proceedings of the IEEE/CVF conference on computer vision and pattern recognition*, 2018.
- [42] X. Wen, P. Xiang, Z. Han, Y.-P. Cao, P. Wan, W. Zheng, and Y.-S. Liu, "Pmp-net: Point cloud completion by learning multi-step point moving paths," in *Proceedings of the IEEE/CVF conference on computer vision and pattern recognition*.
- [43] X. Wang, M. H. Ang, and G. Lee, "Cascaded refinement network for point cloud completion with self-supervision," *IEEE Transactions on Pattern Analysis and Machine Intelligence*, 2021.
- [44] Y. Liu, J. He, X. Chen, Z. Zhang, H. Zhao, C. Dong, and Y. Qiao, "Very lightweight photo retouching network with conditional sequential modulation," *arXiv preprint arXiv:2104.06279*, 2021.
- [45] A. Geiger, P. Lenz, and R. Urtasun, "Are we ready for autonomous driving? the kitti vision benchmark suite," in *Proceedings of the IEEE/CVF conference on computer vision and pattern recognition*. IEEE, 2012.